

FLUID DYNAMICS ANALYSIS OF A COUNTER ROTATING DUCTED PROPELLER

Chao Xu, Cees Bil, Sherman CP. Cheung
School of Aerospace, Mechanical and Manufacturing Engineering, RMIT University

Keywords: *Twin counter-rotating propellers, ducted propellers, RANS, CFD*

Abstract

The use of ducted propellers is common in VTOL UAV design. The presence of a duct improves propeller efficiency, provides protection and improves safety. The aim of this paper is to employ a sensitivity study for the total thrust of a ducted twin counter-rotating propeller system design for UAV applications using computational fluid dynamics. Two factors were investigated: propeller spacing and difference between blades pitch angle. Using 4 discrete values for both factors, 16 designs were analyzed and evaluated. The same approach was used for an equivalent unducted propeller system to assess the influence of the duct.

A ducted twin counter-rotating propeller system was modeled in ANSYS CFX. Shear Stress Transport (SST) turbulence model was used for steady state simulations. An unstructured mesh with prism boundary layers was generated for the computational domains. It was found that the total thrust of both open and ducted counter-rotating propeller is highly dependent on the difference between blade pitch angles and propeller spacing. In terms of total thrust, the presence of a duct did not always improve system performance of counter-rotating propellers.

Symbols

A	Area of rotor disk	[m ²]
A _e	Diffuser exit plane area	[m ²]
D	Diameter of the propeller	[cm]
h ₀	First layer height	[m]
S	Propellers spacing	[cm]
T _{total}	Total thrust of the propulsion system	[N]
U _∞	Freestream velocity	[m / s]
y ⁺	Non-dimensional wall distance	[-]
α	Angle of attack	[deg]
β _F	Front blade local pitch angle	[deg]

β _R	Rear blade local pitch angle	[deg]
σ _d	Diffuser expansion ratio	[-]
Δθ _i	Difference between blades pitch angle	[deg]

1 Introduction

One of the most successful VTOL UAV for surveillance tasks is the Honeywell T-hawk shown in Fig. 1 [1]. The main characteristic of the T-hawk is the ducted fan as the propulsion system. Ducted fans or propellers improve the total thrust in hover condition [2]. The rotation of propeller creates a suction pressure gradient on shroud inlet surface. The duct also provides protection to the propellers and the UAV operator. Another application in VTOL UAV design are twin counter rotating propellers to cancel out the torque. This technique is also used in some helicopters.



Fig. 1. Honeywell's T-Hawk [1]

A VTOL UAV design with two counter-rotating ducted propellers is shown in Fig. 2. Previous

research has studied different duct shapes. The diffuser shape of duct is the key factor improving the total thrust for single ducted propeller [4]. The diffuser section of the duct restrains the natural contraction of the air flow passing through the propeller. The principle shroud parameters affecting shrouded-rotor performance is shown in Fig. 3. In addition a short-shroud coaxial concept was highlighted in previous research [5]. In this research the characteristic of short-shroud with exit diffuser was adopted. A schematic diagram with the main dimensions is shown in Fig. 4.

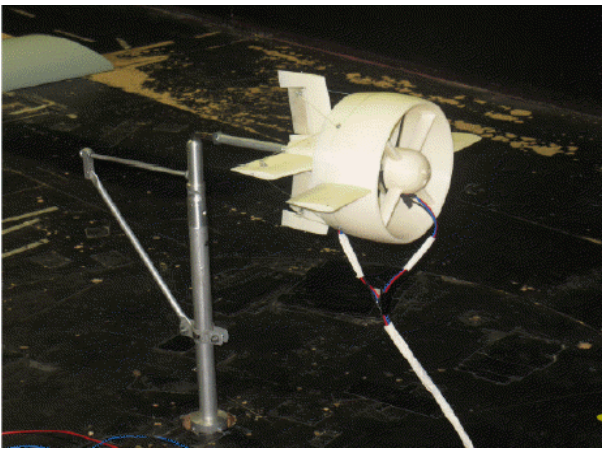


Fig. 2. VTOL UAV prototype in wind tunnel test [3]

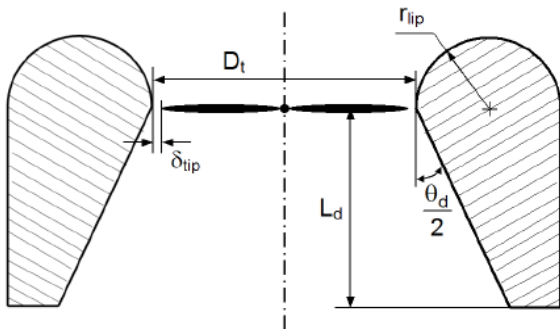


Fig. 3. Principal shroud parameters affecting shrouded-rotor performance [4]

The purpose of this study is to determine the effect of propeller spacing and difference between the rear blade pitch angle and front blade pitch angle on total thrust. ANSYS CFX was used to model the system and evaluate the total thrust.

The definition of propeller spacing is the distance between roots of the propellers. The propeller spacing (S) is one of the fundamental components of the twin counter-rotating propeller system which has been tested due to

the associated aerodynamic effects. The diameter of the propeller (D) is 24 cm. Propeller spacing with 5 cm is the constraint which keeps both propellers operating with small tip clearance. Four discrete propeller spacings were chosen from 3.5 cm to 5 cm, with 0.5 cm increment. The S/D ratio is used as a non-dimensional parameter. The S/D ratios are from 0.146 to 0.208.

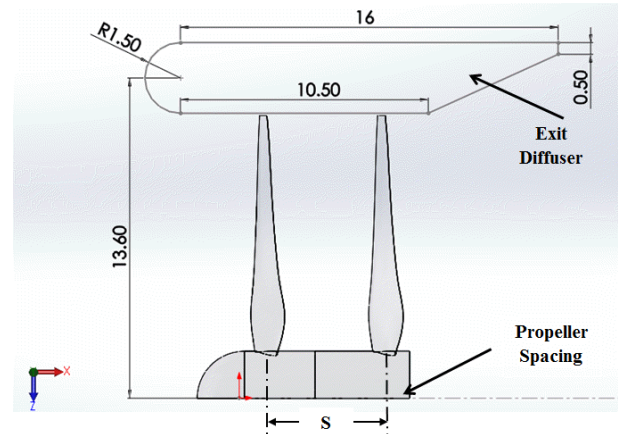


Fig. 4. Propeller spacing and duct configuration in CAD (Dimensions are in cm)

The other factor is the difference between blades pitch angle ($\Delta\theta_i$). The geometry definition is shown in Fig. 5. The $\Delta\theta_i$ value is constant along the blade, i.e. the blade twist distribution is the same for both propellers.

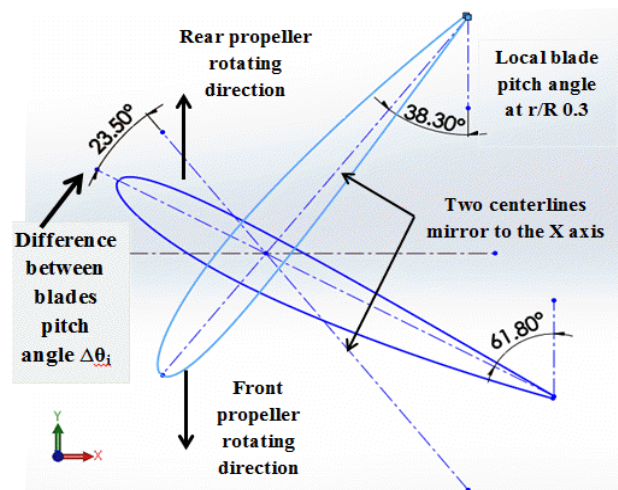


Fig. 5. Definition of the difference between blades pitch angle $\Delta\theta_i$ (23.5 degree example) and the relation to the local blade pitch angles of both propeller blades at r/R 0.3 cross section

According to Lee [6], the local blade pitch angle distributions of the front and rear propeller are related. The rear propeller in general requires a greater blade pitch compared to that of the front

propeller, because the rear propeller works in the wake generated by the front propeller and therefore needs more torque. In this sensitivity study, 4 values of $\Delta\theta_i$ were selected from 1.5 to 67.5 degree, with 22 degree step as shown in Fig. 6.

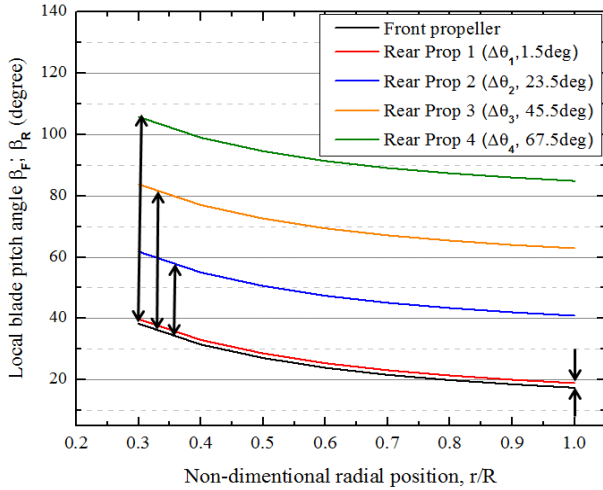


Fig. 6. Four values of difference between blades pitch angle

2 Model Geometry and Configurations

JavaFoil, JavaProp and SolidWorks were the main software tools used in the design process of duct and propellers.

2.1 Propeller design

JavaProp is a tool for the design and the analysis of propellers. The method is based on blade-element-momentum theory [7]. The design process is shown in Fig. 7 [8].

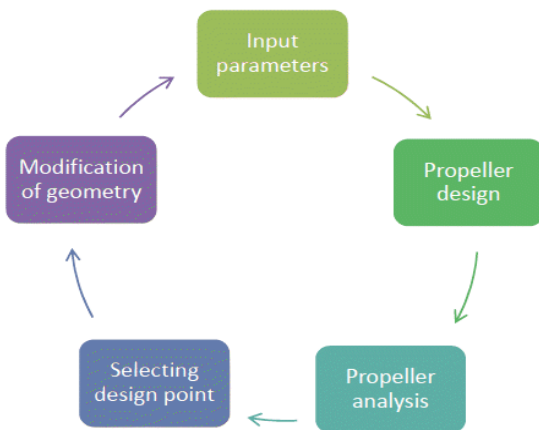


Fig. 7. Flow chart of design process [8]

The number of the blades is two. The design propeller speed is 10,000 rpm. In hover, the maximum tip speed for the propeller was 125.7 m/s, which equal to a tip Mach number 0.36 at sea level ISA condition, so compressibility effects were ignored. Another design parameter that must be specified is the desired thrust in cruise speed or available shaft power. The available power in hover is about 300 W.

Another part of the design process is to select the airfoil distribution and lift to drag ratio. A single airfoil was used for simplicity. In this research NACA 2412 airfoil was selected as the cross section airfoil of the blade.

The lift to drag ratio, as calculated by JavaFoil was around 44.2 to 47.7. JavaFoil implements a panel method to determine the linear potential flow field around airfoils [9]. The airfoil polar is exported into JavaProp in standard XML format. JavaProp provides the chord length and blade angle distributions based on the direct inverse design module for maximum efficiency [7]. The shape of the propeller from JavaProp is viewed in Fig. 8.

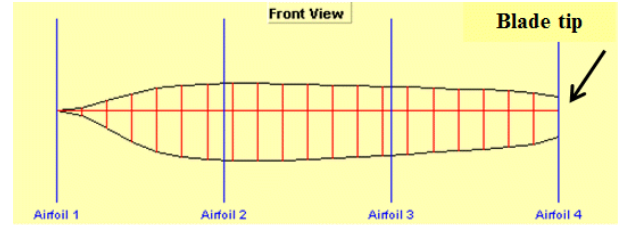


Fig. 8. Chord length distribution along the radius in front views from JavaProp

The aforementioned method did not consider the spinner of propeller. The radius of spinner is set as 2cm. there is an overlapped region between the spinner and origin designed propeller. Therefore, both chord length and blade angle adopt JavaProp results from 2 cm to 12 cm in radius direction.

A blunt configuration was used near the blade root to make the shape of propeller in this paper similar to a normal propeller, which is shown in Fig. 9. The CAD model of the front propeller is built in Fig. 10.

The aerodynamic portion of the blade starts from non-dimensional radial position at 0.3. The rear blade keeps the same chord distribution as from the front blade. One of the targets of the

research is to investigate effect of $\Delta\theta_i$ on the total thrust value in hover. Generally the local blade pitch angle of the rear propeller (β_R) is related to that of the front propeller:

$$\beta_R = \beta_F + \Delta\theta_i \quad (1)$$

The local blade pitch angle distribution of front propeller (β_F) is shown in Fig. 11. All four rear propeller configurations were modeled in the SolidWorks.

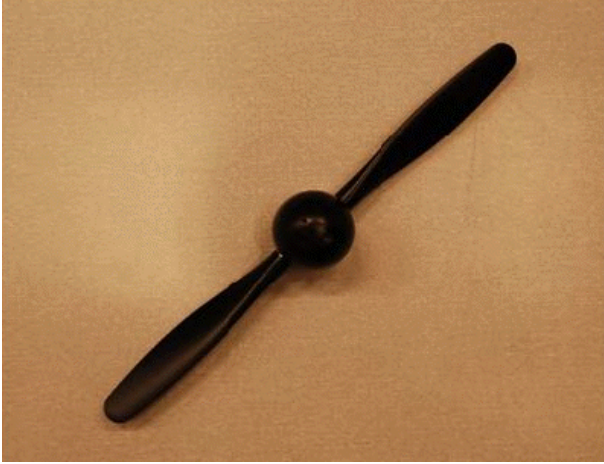


Fig. 9. The Beaver propellers [10]

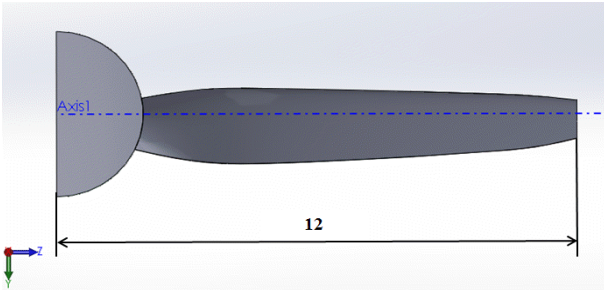


Fig. 10. The front propeller configuration with spinner CAD model (Dimensions are in cm)

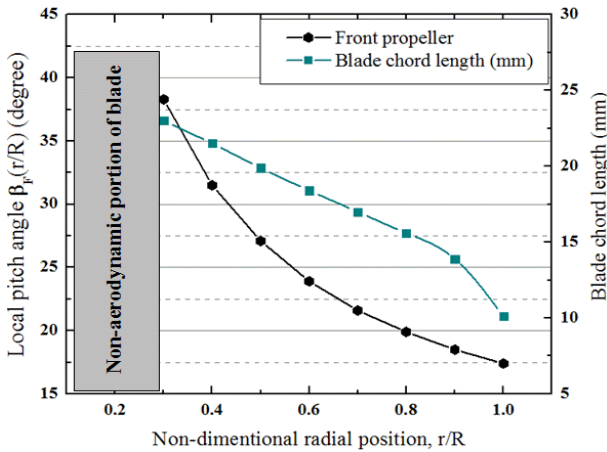


Fig. 11. Local blade pitch angle β_F and chord length distributions of the front propeller

2.2 Duct

The effect of the duct has always been attractive for the designer, because the duct can ruggedize the rotor system, improve propeller efficiency and protect the propeller. The application is also used in wind turbines, tidal turbines, and marine propellers [11, 12, 13]. Ducts used in wind turbines aim to increase the power [11]. The objective of this study is to increase the static thrust for a UAV application in this research. Single ducted propellers with small tip clearance show an advantage of thrust increase in the hover condition, because the rotation of propeller creates a suction pressure gradient on the shroud inlet surface.

Previous research studied different duct shapes and relative propeller positions for a single ducted propeller. Pereira [4] highlights the shape of the duct as a diffuser and introduces a key parameter for determining the performance diffuser expansion ratio σ_d , which is equal to the ratio of the diffuser exit plane area A_e to the area of the rotor disk A :

$$\sigma_d = A_e/A \quad (2)$$

$$T_{total} = T_{rotor} + T_{duct} \quad (3)$$

In addition, in the hover condition the total system thrust includes rotor thrust and duct thrust. The duct thrust is made of inlet and diffuser components. These two components are functions of the diffuser expansion ratio. In this research a diffuser duct was used and the shape of cross section is shown in Fig. 4.

According to the definition of the diffuser expansion ratio, the ratio is about 1.48. The relative position of the front propeller is fixed and propeller spacing varies with four discrete values.

3 Numerical Method

In this section, the application of CFX is described in detail, including the mesh generation process and the numerical steps followed for different runs.

3.1 Single propeller

For all simulations the flow in the control volume was treated as air at 25 °C under 1.01325×10^5 Pa reference pressure. An inlet normal speed boundary was imposed in the propeller axial direction. In hover condition the U_∞ was assumed as 0 m/s at an angle of attack α of 0°. The boundary condition at outlet was set as average static pressure, which is 0 Pa relative to the reference pressure. Pressure outlet boundary interpreted the flow exhausts into the atmospheric static pressure of environment. The control volume was divided into an inner and outer domain. Half of the cylinder domain was built because of symmetry of the propeller. The inner domain includes the hub and blade configuration as shown in Fig. 12. The diameter of the inner domain is slightly larger than that of the propeller. The outer domain covers the shaft, as shown in Fig. 13.

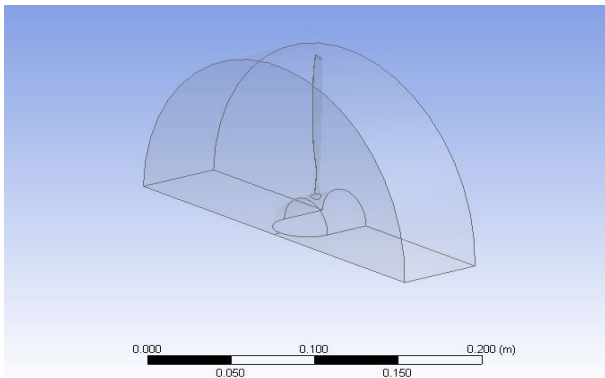


Fig. 12. Inner rotating domain

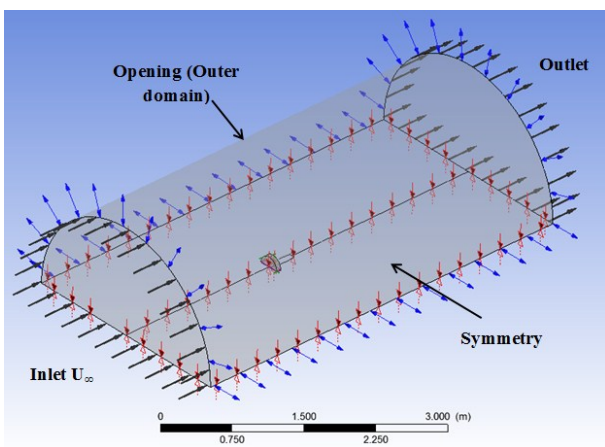


Fig. 13. Outer stationary domain

Multiple reference frames (MRF) was used in this study. The MRF model allows for the subdomains which require rotating velocity

inputs. In this study a steady state approximation was used where the fluid zone in the propeller region is modeled as a rotating frame of reference and the outer zone is modeled in a stationary frame. The total length of the outer domain is 20 times diameter of propeller, which is 4.80 m. The height of the outer domain is 1.32 m.

Boundary conditions are imposed by defining: constant inflow velocity; opening with relative pressure 0 Pa; zero gauge pressure at outlet and no slip wall at solid surface of blade. Interface includes frozen-rotor for the regions change. The Frozen Rotor model treats the flow in MRF model from rotating domain to stationary one and maintains their relative position [14].

In terms of mesh types, an unstructured mesh was chosen for both domains. The mesh is generated by applying the inflation method. The aim of using the inflation method is to produce prismatic mesh element for the boundary layers and increase the resolution in the region [14]. The inflation method can be used to obtain non-uniform grids. The employment of non-uniform grids allows the grid to be more refined in regions where strong gradients are expected.

The volume attached to the surface is composed of prism layers. First layer thickness was chosen for the grids near the solid wall in order to resolve the viscous region of flow. The layers consist of 10 single layers with 1.05 growth rate. The non-dimensional wall distance (y^+) is a critical parameter for inflation mesh requirements. In theory in order to resolve the viscous sub-layer y^+ is smaller than 5. The simulation is performed by using the SST turbulence model [15]. In this study non-dimensional wall distance y^+ less than 1 was achieved near the solid wall for the counter-rotating blades and duct.

In order to achieve the small y^+ , the first layer height h_0 is set as 6.5×10^{-7} m. Further element size for coarse mesh is set 6.5×10^{-3} m in the inner domain. The inner domain mesh can be viewed in Fig. 14. Compared with the inner domain, the outer domain has a lower mesh elements density. The total number of final mesh elements including both inner and outer domain reaches 3.5 million. The average

skewness value of mesh is 0.257. In according with the relationship between cell skewness and quality [16]: the quality of the mesh is good.

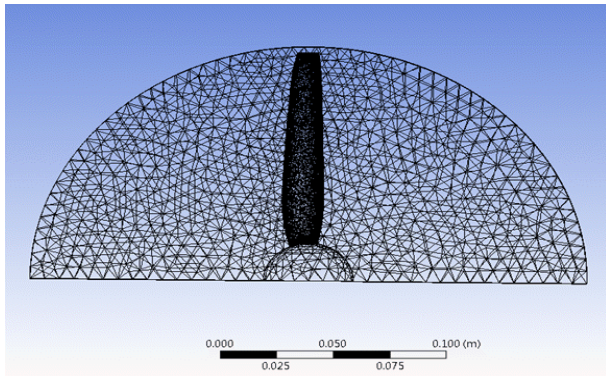


Fig. 14. Coarse grid of inner rotating domain

All numerical results were obtained by solving the Navier-Stokes equation through the SST turbulence model. Steady state simulation was selected. In terms of the solver setup a High Resolution Scheme is employed for calculating the advection term in the discrete finite volume equations [17]. A physical timestep of 1.0×10^{-3} seconds is used [14]. Thrust force is monitored by using CFX Expression Language in the axial direction. A grid independence study was employed by using the same surface meshes and increasing the element number by size control. Grid independence study was determined by comparing a mesh with 3.5 million, 4.2 million and 5.3 million cells, respectively. It shows that the change in thrust is less than 1.0% as the number of elements increase from 4.2 to 5.3 million. This suggests that the medium mesh is adequate for this study. CFX predicted the thrust of isolated front propeller as 12.66 N in hover.

3.2 Open counter-rotating propellers

In this part the difference of domain and solver setting is highlighted between single and counter-rotating propellers. The outer boundary conditions are the same. The difference is the inner domain. In the open counter-rotating propeller simulation the inner domain includes two counter-rotating disks. The S/D ratio is small. Therefore the counter-rotating domains are connected, as shown in Fig.15.

The interface between counter-rotating domains is also set as frozen rotor. To investigate the

effect of propeller spacing on thrust the front blade is fixed and rear propeller changes to achieve the different spacing. One of the drawbacks of using the steady state simulation is that it may not fully capture the unsteady interaction effects between front and rear propeller.

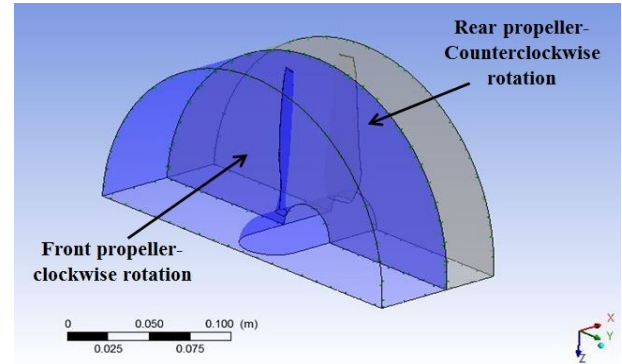


Fig. 15. Inner domain in open counter-rotating propeller simulation

The total thrust in hover with 3.5 cm propeller spacing and $\Delta\theta_1$ reaches 17.51 N. As the spacing increased from 3.5 cm to 5 cm total thrust increased by 1.03 N. With propeller spacing 5 cm as the $\Delta\theta_1$ increased from 1.5 degree to 23.5 degree the total thrust reached the highest value, which is 26.4 N, as shown in Fig.16. Then the total thrust decreased as $\Delta\theta_1$ increased to 67.5 degree. The $\Delta\theta$ effect on total thrust with other propeller spacings is nearly the same. Within $\Delta\theta_2$ condition the propeller spacing effect on total thrust was initially evident from 3.5 cm to 4.5 cm then no apparent improvement as the spacing increasing to 5 cm.

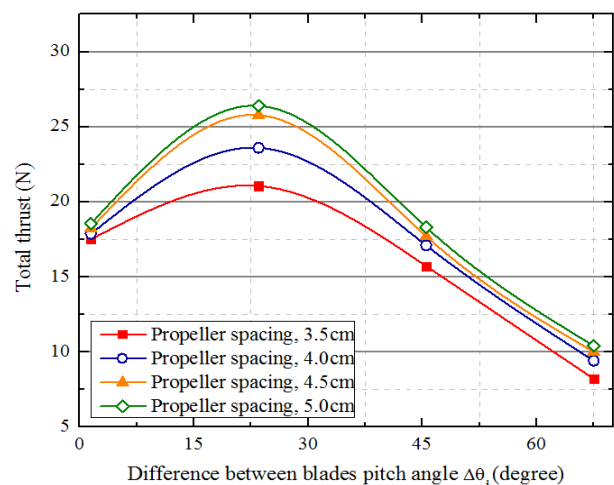


Fig. 16. Open counter-rotating propeller total thrust in hover

3.3 Ducted counter-rotating propellers

The aim of the diffuser duct is to reduce the tip loss of both propellers. Ducts with a single rotor have been analyzed through numerical method in previous research [18]. Here we focus on a duct with two counter-rotating propellers. In the simulation process the configuration of the duct is added into the inner domain shown in Fig. 17.

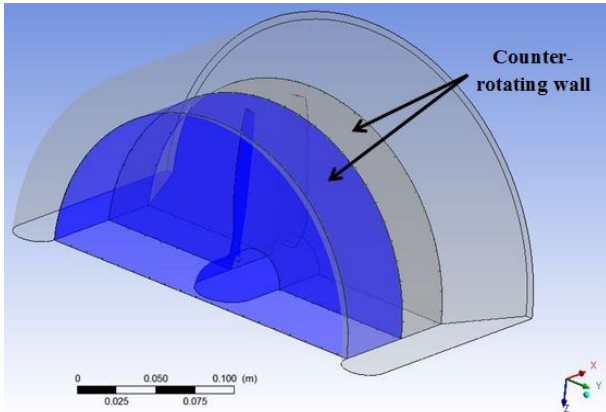


Fig. 17. Inner domain for duct counter-rotating propeller application

The surface of rotating domain connects with the inner surface of the duct. Therefore, the radius of rotating domain needs to be modified. The interface between the duct and propeller domain is treated as a counter-rotating wall [19]. The simulation is also concerned about total thrust, including the duct component in hover condition. Propeller spacing and $\Delta\theta$ effects on total thrust are shown in Fig.18.

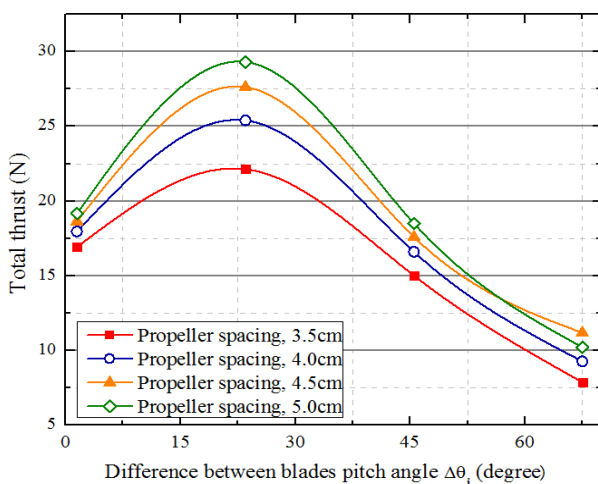


Fig. 18. Ducted counter-rotating propeller total thrust in hover

Changing the $\Delta\theta_i$ values has nearly the same effects on the total thrust in duct counter-

rotating propellers compared with open counter-rotating propeller. The maximal total thrust was also gained with $\Delta\theta_2$ with varied propeller spacings. But the spacing effect is different with $\Delta\theta_4$. The thrust of ducted counter-rotating propellers decreased as the propeller spacing increased from 4.5cm to 5cm.

4 Conclusions and Outlook

This paper presents a sensitivity study of the total thrust of a ducted counter-rotating propeller configuration with respect to propeller spacing and the difference between blades pitch angle. ANSYS CFX was used for geometry meshing and analysis. It was shown that increasing the propeller spacing within selected range increases the total thrust for open counter-rotating propellers. At fixed propeller spacing there is a maximal thrust with $\Delta\theta_2$. Unlike single ducted propeller, which always improves the thrust performance to isolated propeller with small tip clearance, only with $\Delta\theta_2$ ducted counter-rotating propeller improved at higher level upon the performance of total thrust compared with open one in hover. With $\Delta\theta_1$ and 3.5 cm propeller spacing the ducted counter-rotating propeller produced lower thrust than without duct. As the spacing increase from 4cm to 5cm, the total thrust is slightly higher than the equivalent open counter-rotating system. With $\Delta\theta_3$ the system suffered performance degradations compared with open counter-rotating propellers except 5 cm propeller spacing. With $\Delta\theta_4$, only 4.5 cm propeller spacing experienced total thrust improvement. From CFD perspective, the results were calculated by using the steady state simulation. One of the drawbacks is that it did not fully capture the unsteady interaction effects between front and rear propeller. In further research the unsteady simulation will be performed and there also needs the experiment validation assessment for the numerical method.

References

- [1] Honeywell T-Hawk, Honeywell Aerospace, <http://aerospace.honeywell.com/products/unmanned-aerial-sysems/t-hawk-mav> [Retrieved: March 3, 2014]

- [2] Martin P and Tung C. Performance and flowfield measurements on a 10-inch ducted rotor VTOL UAV, *American Helicopter Society 60th Annual Forum Proceeding*, Baltimore, MD, June 7-10, 2004.
- [3] Zhao H W. *Development of a dynamic model of a ducted fan VTOL UAV*, Master. Thesis, RMIT University, 2009.
- [4] Pereira J L. *Hover and wind-tunnel testing of shrouded rotors for improved micro air vehicle design*, Ph.D. thesis, University of Maryland, 2008.
- [5] Grondin G, Thipyopas C and Moschetta J M. Aerodynamic Analysis of a Multi-Mission Short-Shrouded Coaxial UAV: Part III – CFD for Hovering Flight, *AIAA Applied Aerodynamics Conference*, Chicago, Illinois, 28 June-1 July 2010.
- [6] Lee T E. *Design and performance of a ducted coaxial rotor in hover and forward flight*, Master. Thesis, University of Maryland, 2010.
- [7] Hepperle M. JavaProp User's Guide, 2013.
- [8] Kodiyattu S T. *Design of a propeller for downwind faster than the wind vehicle*, Master. Thesis, San Jose State University, 2010.
- [9] Hepperle M. JavaFoil User's Guide, 2011.
- [10] Dimchev M., Experimental and numerical study on wingtip mounted propellers for low aspect ratio UAV design, Master. Thesis, Delft University of Technology, 2012.
- [11] Ten Hoopen P.D.C. *An experimental and computational investigation of a diffuser augmented wind turbine; with an application of vortex generators on the diffuser trailing edge*, Master. Thesis, Delft University of Technology, 2009.
- [12] Consul A Claudio. *Hydrodynamic analysis of a tidal cross-flow turbine*, Ph.D. Thesis, University of Oxford, 2011.
- [13] Park W G., Jung Y R and Kim C K. Numerical flow analysis of single-stage ducted marine propulsor, *Ocean Engineering*, Vol.32, pp. 1260-1277, 2005.
- [14] ANSYS, Inc., *ANSYS CFX Reference Guide Release 14.0*, 2011
- [15] Menter F R. Two-equation eddy-viscosity turbulence models for engineering applications. *AIAA Journal*, Vol. 32, No. 8, pp. 1598-1605, 1994.
- [16] ANSYS, Inc., *Meshing-Help 12.0*, 2009.
- [17] ANSYS, Inc., *ANSYS CFX-Solver Modeling Guide 14.0*, 2011.
- [18] Lakshminarayan V K and Baeder J D. Computational investigation of microscale shrouded rotor aerodynamics in hover, *Journal of the American Helicopter Society*, Vol. 56, No.4, pp. 1-15, 2011.
- [19] Thouault N, Breitsamter C and Adams N A. Numerical Investigation of Inlet Distortion on a Wing-Embedded Lift Fan. *Journal of Propulsion and Power*, Vol. 27, No.1, pp. 16-28, 2011.

Contact Author Email Address

Chao Xu: xc1986xcxc@gmail.com

Copyright Statement

The authors confirm that they, and/or their company or organization, hold copyright on all of the original material included in this paper. The authors also confirm that they have obtained permission, from the copyright holder of any third party material included in this paper, to publish it as part of their paper. The authors confirm that they give permission, or have obtained permission from the copyright holder of this paper, for the publication and distribution of this paper as part of the ICAS 2014 proceedings or as individual off-prints from the proceedings.